2009 IEEE International Conference on Robotics and Automation
Kobe International Conference Center
Kobe, Japan, May 12-17, 2009

A Stochastically Stable Solution to the Problem of Robocentric Mapping

Adrian N. Bishop and Patric Jensfelt

***Abstract*— This paper provides a novel solution for robocentric mapping using an autonomous mobile robot. The robot dynamic model is the standard unicycle model and the robot is assumed to measure both the range and relative bearing to the landmarks. The algorithm introduced in this paper relies on a coordinate transformation and an extended Kalman filter like algorithm. The coordinate transformation considered in this paper has not been previously considered for robocentric mapping applications. Moreover, we provide a rigorous stochastic stability analysis of the filter employed and we examine the conditions under which the mean-square estimation error converges to a steady-state value.**

I. Introduction

Simultaneous localization and mapping (or SLAM) refers to the process of building a map of an environment from sensory information gathered by a mobile robot, while simultaneously estimating the position of the robot using the map [1]–[6]. An introduction to the SLAM problem is available in many papers; e.g. see [7], [8] and the references therein for an overview of the different approaches. Following the work in [1], one of the most common methods for solving the SLAM problem is to use an extended Kalman Filter (EKF). However, the traditional SLAM state vector[1] [1], [2], [4] in a global coordinate system is not observable as discussed in [9] given only relative landmark-robot measurements such range and/or bearing. Another problem is that of estimator inconsistencies caused by accumulated linearization errors [10]–[12]. In [13] the concept of robocentric mapping is introduced and this concept it is shown to better deal with linearization errors than the traditional SLAM formulation.

The EKF consistency and the convergence of the approximate EKF covariance matrix is analyzed in [12] for the general problem of SLAM. However, it is possible, in the framework of the EKF, for the covariance matrix to be asymptotically bounded while the state estimation error diverges asymptotically. Moreover, it is the state estimate itself that will be used by the robot when making decisions etc. Hence, the actual (or mean) estimation error is a more meaningful quantity to analyze.

The primary contribution of this paper is the development of a robocentric mapping algorithm based on a simple, yet particularly important, coordinate transformation. By building a map in a relative polar framework we eliminate the nonlinearities associated with the measurement equation. Moreover, we eliminate the difficulties associated with the unobservable states [9] and the inconsistencies caused by the affect of the EKF linearizations (which alter the unobservable subspace [9]). A robocentric map is also (arguably) more useful/natural than a global map for a large class of problems. The relative robot dynamic model remains nonlinear but takes on a different form. We then apply the standard extended Kalman filter (EKF) to this problem and justify this approach via a rigorous stochastic convergence analysis. The convergence of the EKF relative map is given in terms of the mean estimation error and is based on stochastic calculus. The convergence analysis in this paper is necessarily conservative, with the particular asymptotic properties of the mean estimation error being naturally dependent on the exact robot trajectory; e.g. see [14]–[18].

The approach and analysis given in this paper was partly inspired by [9][13] where the difficulties of the global SLAM problem are highlighted and where it is implied (perhaps not always explicitly) that a robocentric approach would circumvent many of these problems. The coordinate framework chosen in this paper was inspired by the large bearing-only tracking literature where it is shown that removing the nonlinearities associated with the measurement equation can significantly improve the EKF performance [19], [20]. Finally, a rigorous mean-error convergence analysis was given to further justify the application of the EKF and to provide a deeper insight into the proposed robocentric mapping algorithm.

The remainder of this paper is organized as follows. In Section II we introduce some preliminary notation and conventions. In Section III we introduce the concept of mapping in polar coordinates using a robocentric framework. We outline the standard extended Kalman filter-like algorithm which forms the basis of the estimator considered in this paper. In Section III we then analyze the observability of the mapping problem considered and the convergence properties of the particular estimator considered. In Section IV we present some simple simulation results and in Section V we relate our robocentric problem to the traditional SLAM problem. In Section VI we give our conclusions.

II. Preliminaries

Consider a single robot with a state $\mathbf{s}_r = [x_r \ y_r \ \phi_r]^\top \in \{\mathbb{R}^2 \times \mathbb{SO}(1,\mathbb{R})\}$ where x_r and y_r are the robot's Cartesian position coordinates and ϕ_r is the robot's heading. The robot dynamics are based on the unicycle model,

$$\begin{aligned} \dot{x}_r &= v_r \cos\phi_r \\ \dot{y}_r &= v_r \sin\phi_r \\ \dot{\phi}_r &= w_r \end{aligned} \tag{1}$$

A.N. Bishop and P. Jensfelt are with the Centre for Autonomous Systems, KTH, Stockholm, Sweden. This work was supported by the Centre for Autonomous Systems (CAS) and the EU FP7 project CogX.

[1]The traditional SLAM state vector consists of the pose of the robot and the Cartesian location of the landmarks.

978-1-4244-2789-5/09/$25.00 ©2009 IEEE

where v_r is the translational velocity and w_r is the robots angular velocity. Note that there are three robot state variables in $\{\mathbb{R}^2 \times \mathbb{SO}(1, \mathbb{R})\}$ and only two control inputs. The nonholonomic constraint on the robot is given by

$$\dot{x}_r \sin\phi_r = \dot{y}_r \cos\phi_r \tag{2}$$

The robot will generally only know v_r and w_r up to some error denoted by v and w respectively. Here, v and w are assumed to be uncorellated zero-mean Weiner processes. The dynamics of the robot are thus assumed to obey

$$d\begin{bmatrix} x_r \\ y_r \\ \phi_r \end{bmatrix} = \begin{bmatrix} v_r\cos\phi_r \\ v_r\sin\phi_r \\ w_r \end{bmatrix} dt + \begin{bmatrix} \sigma_v\cos\phi_r & 0 \\ \sigma_v\sin\phi_r & 0 \\ 0 & \sigma_w \end{bmatrix}\begin{bmatrix} dv \\ dw \end{bmatrix} \tag{3}$$

which is a stochastic differential equation of the Ito-type. Here, σ_v and σ_w are the standard-deviations of the errors v and w respectively. The environment is populated with a set $\mathcal{V}$ of landmark (or feature) points with $|\mathcal{V}| = n$. The Cartesian position of the i^{th} landmark is denoted by $\mathbf{p}_i = [x_i \ y_i]^\top \in \mathbb{R}^2$. The landmarks are stationary in this case and represent the map of the environment which is to be estimated by the mobile robot. At some time t the robot can sense a subset $\mathcal{G}(t) \subseteq \mathcal{V}$ of landmarks. At time t the true robot measurements are given by

$$\begin{aligned} d_i &= \sqrt{(x_i - x_r)^2 + (y_i - y_r)^2} \\ \vartheta_i &= \theta_i - \phi_r = \arctan\left(\frac{y_i - y_r}{x_i - x_r}\right) - \phi_r \\ & \quad \forall i \in \mathcal{G}(t) \end{aligned} \tag{4}$$

where $\vartheta_i = \theta_i - \phi_r$ is the relative bearing to i^{th} landmark in the robots internal Cartesian coordinate system, i.e. the Cartesian coordinate system rotated by the robots heading. Let $\mathbf{z} = [\mathbf{s}_r \ \mathbf{p}_i \ \ldots \ \mathbf{p}_n]^\top$ denote a traditional SLAM state vector. The measurements are typically corrupted by a noise process $\mathbf{n}(t)$ such that

$$d\mathbf{y}(t) \triangleq \psi dt = h(\mathbf{z})dt + \mathbf{E}(t)\mathbf{n}(t) \tag{5}$$

in continuous-time. Here, $\mathbf{n}(t)$ is a zero-mean Weiner process and $\mathbf{E}(t)$ is a measurement noise weighting matrix that can be dependent on the true state. The measurements and robot dynamics are nonlinear in the chosen coordinate system.

III. Improved Robocentric Mapping in Polar Coordinates

The contribution of this paper is a novel robocentric algorithm for mapping and localization that takes advantage of the polar-like nature of the relative range and bearing measurements. There does not appear to be any similar (polar-like) algorithms in the SLAM or robocentric mapping literature. However, there is a long history in the bearing-only tracking literature [19], [20] of working in variants of polar coordinate systems. The motivation is that the measurements are then linear in the state components. Recall the measurements taken by the robot are in the form

$$\begin{aligned} d_i &= \sqrt{(x_i - x_r)^2 + (y_i - y_r)^2} \\ \vartheta_i &= \theta_i - \phi_r = \arctan\left(\frac{y_i - y_r}{x_i - x_r}\right) - \phi_r \end{aligned} \tag{6}$$

where the state $\mathbf{s}_r = [x_r \ y_r \ \phi_r]^\top$ of the robot and the position of the landmarks $\mathbf{p}_i = [x_i \ y_i]^\top \in \mathbb{R}^2$ are in some external (non-robocentric) coordinate system. The measurements are nonlinear in the first two components of $\mathbf{s}_r$ and in $\mathbf{p}_i$, $\forall i$.

Now define the following state variable $\mathbf{r}_i = [d_i \ \vartheta_i]^\top$ with $d_i \in (0, \infty)$ and $\vartheta_i \in [-\pi, \pi)$. The augmented state variable in this section is given by $\mathbf{z} = [\mathbf{r}_1 \ \ldots \ \mathbf{r}_n]^\top$. The measurements (6) are linear in $\mathbf{r}_i$ or more generally in $\mathbf{z} = [\mathbf{r}_1 \ \ldots \ \mathbf{r}_n]^\top$ and are given by the continuous-time measurement equation

$$d\mathbf{y}(t) \triangleq \psi dt = \mathbf{H}(\mathcal{G}(t))\mathbf{z}dt + \mathbf{E}(t)\mathbf{n}(t) \tag{7}$$

where $\mathbf{E}(t)$ is not required to be independent of $\mathbf{z}$. Here, $\mathbf{H}(\mathcal{G}(t))$ is a time-varying linear matrix which is dependent only on the set $\mathcal{G}(t)$ of currently sensed landmarks. For example, if all of the landmarks are sensed and the state variable $\mathbf{z}$ is ordered appropriately, then $\mathbf{H}$ would be the identity matrix.

Consider again a robot that obeys the unicycle model (1) in $\mathbb{R}^2 \times \mathbb{SO}(1, \mathbb{R})$. Then we can write down the following differential equation for the dynamics of $\mathbf{r}_i$,

$$\begin{aligned} \dot{d}_i &= -v_r\cos\vartheta_i \\ \dot{\vartheta}_i &= \frac{v_r}{d_i}\sin\vartheta_i - w_r \end{aligned} \tag{8}$$

which is nonlinear in $\mathbf{r}_i$. Note also that d_i must be bounded away from zero. Again we (must) assume that the control inputs are corrupted by an additive noise process v and w such that

$$\begin{aligned} d\begin{bmatrix} d_i \\ \vartheta_i \end{bmatrix} &= \begin{bmatrix} -v_r\cos\vartheta_i \\ \frac{v_r}{d_i}\sin\vartheta_i - w_r \end{bmatrix} dt + \\ & \begin{bmatrix} \sigma_v\cos\vartheta_i & 0 \\ \sigma_v\sin\vartheta_i & -\sigma_w \end{bmatrix}\begin{bmatrix} dv \\ dw \end{bmatrix} \end{aligned} \tag{9}$$

is a more accurate depiction of the relative robot and i^{th} landmark dynamics. Here, v and w are uncorellated Weiner processes with standard deviations of σ_v and σ_w respectively. Note that the affect of v on ϑ_i and d_i is conditioned on a nonlinear function of a true state variable (in this case ϑ_i).

A. On the Observability of the Polar SLAM Problem and the Convergence of the EKF-Based Polar SLAM Algorithm

In this subsection we will examine and prove a number of results related to the observability of the considered polar-coordinate SLAM problem formulation. We will also examine and prove a number of results regarding the convergence of an EKF-like algorithm for estimating the relative polar state variable.

1) Error Free Measurements and Dynamics: We consider first the observability properties of the state $\mathbf{z} = [\mathbf{r}_1 \ \ldots \ \mathbf{r}_n]^\top$ with $\mathbf{r}_i = [d_i \ \vartheta_i]^\top$ evolving according to (8). We also assume error free measurements of the form

$$\psi dt = \mathbf{H}(\mathcal{G}(t))\mathbf{z}dt \tag{10}$$

such that the system and measurements are noiseless and deterministic. The following result concerns the observability of the subspace $\mathbf{r}_i = [d_i \ \vartheta_i]^\top$ for some $i \in \mathcal{V}$.

Corollary 1: Assume the robot-landmark dynamics and the measurements are deterministic and error free. The state $\mathbf{r}_i(s) = [d_i(s)\ \vartheta_i(s)]^\top$ for some $i \in \mathcal{V}$ and for $s \geq \tau$ or $s < \tau$ can be calculated at any time $t \geq \tau$ if and only if $\mathcal{G}(\tau) \cap \mathbf{r}_i(\tau) \neq \emptyset$ for some instant τ.

The fact that Corollary 1 is true is not surprising. However, it again highlights the observable space of the SLAM problem is purely relative [9]. Hence, by considering a relative (robocentric) mapping algorithm we are not attempting to extract more information (in any finite time) from the measurements than is available [9][12].

2) Error Free Dynamics and Noisy Measurements: A natural extension to the above result concerns the behavior of an estimate $\widehat{\mathbf{z}}$ of $\mathbf{z}$ when the dynamics of the state $\mathbf{r}_i = [d_i\ \vartheta_i]^\top$ are error free and deterministic but the measurements

$$d\mathbf{y}(t) \triangleq \psi dt = \mathbf{H}(\mathcal{G}(t))\mathbf{z}dt + \mathbf{E}(t)\mathbf{n}(t) \tag{11}$$

are corrupted by an additive Weiner process. Naturally, the behavior of any state estimate $\widehat{\mathbf{z}}$ depends on the particular estimator and thus let us consider an estimator of the form

$$d\widehat{\mathbf{z}} = f(\widehat{\mathbf{z}}, v_r, w_r)dt + \mathbf{K}(t)\left(d\mathbf{y}(t) - \mathbf{H}(\mathcal{G}(t))\widehat{\mathbf{z}}dt\right) \tag{12}$$

where the function $f_i(\cdot)$ that captures the dynamics of the subspace $\mathbf{r}_i = [d_i\ \vartheta_i]^\top$ is given by

$$f(\widehat{\mathbf{z}}, v_r, w_r) = \begin{bmatrix} -v_r \cos\vartheta_i \\ \frac{v_r}{d_i}\sin\vartheta_i - w_r \end{bmatrix} \tag{13}$$

where v_r and w_r are again considered as deterministic inputs with no errors. The function $f(\cdot)$ is thus a vertical concatenation of the $f_i(\cdot)$. The gain $\mathbf{K}(t)$ is given by

$$\mathbf{K}(t) = \mathbf{P}(t)\mathbf{H}^\top(\mathcal{G}(t))\mathbf{R}^{-1}(t) \tag{14}$$

and $\mathbf{P}(t)$ is the solution to the following Riccati differential equation

$$\begin{aligned} d\mathbf{P}(t) &= \left[\mathbf{A}(t)\mathbf{P}(t) + \mathbf{P}(t)\mathbf{A}^\top(t) + \mathbf{Q}(t)\right]dt - \\ &\quad \mathbf{P}(t)\mathbf{H}^\top(\mathcal{G}(t))\mathbf{R}^{-1}(t)\mathbf{H}(\mathcal{G}(t))\mathbf{P}(t) \end{aligned} \tag{15}$$

where $\mathbf{Q}$ and $\mathbf{R}$ are positive-definite tuning matrices. Note that $\mathbf{A}(t)$ is the Jacobian of $f(\cdot)$ evaluated at $\widehat{\mathbf{z}}$. The Jacobian $\mathbf{A}_i(t)$ of $f_i(\cdot)$ is given by

$$\mathbf{A}_i(t) = \begin{bmatrix} 0 & -v_r\sin\vartheta_i \\ -\frac{v_r}{d_i}\sin\vartheta_i & \frac{v_r}{d_i}\cos\vartheta_i \end{bmatrix} \tag{16}$$

and is evaluated at $\widehat{\mathbf{r}}_i$ and is dependent on v_r. Note the estimation error $\boldsymbol{\zeta} = \mathbf{z} - \widehat{\mathbf{z}}$ evolves according to

$$\begin{aligned} d\boldsymbol{\zeta} &= \left(\mathbf{A}(t) - \mathbf{K}(t)\mathbf{H}(\mathcal{G}(t))\right)\boldsymbol{\zeta}dt + \\ &\quad \varrho(\mathbf{z}, \widehat{\mathbf{z}}, v_r, w_r)dt - \mathbf{K}(t)\mathbf{E}(t)d\mathbf{n}(t) \end{aligned} \tag{17}$$

where we have used the following Taylor expansion of $f(\cdot)$ about the estimate $\widehat{\mathbf{z}}$,

$$f(\mathbf{z}, v_r, w_r) - f(\widehat{\mathbf{z}}, v_r, w_r) = \mathbf{A}(t)(\mathbf{z} - \widehat{\mathbf{z}}) + \varrho(\mathbf{z}, \widehat{\mathbf{z}}, v_r, w_r) \tag{18}$$

where $\varrho(\mathbf{z}, \widehat{\mathbf{z}}, v_r, w_r)$ accounts for the higher order terms. Recall that $\mathbf{r}_i = [d_i\ \vartheta_i]^\top$ with $d_i \in (0, \infty)$ and $\vartheta_i \in [-\pi, \pi)$ for all t. Then it is clear that the following bound holds

$$\|\mathbf{A}(t)\| = \overline{a} < \infty \tag{19}$$

for all t where for any time-varying matrix $\mathbf{M}(t)$ we assume the following

$$\|\mathbf{M}(t)\| = \sup\{\|\mathbf{M}(t)\| : m_{ij} \in \mathbb{R}\} \tag{20}$$

for all t and for some norm $\|\cdot\|$. For the subsequent analysis, it turns out that the coordinate spatial and temporal scales will play an important role. Hence, at this point let us make the following assumptions.

Assumption 1: The translational velocity of the robot $v_r(t)$ is uppperbounded in any arbitrary coordinate scale such that $v_r(t) \leq \overline{v}$ for all t. For simplicity we also assume that $v_r(t) > 0$ for all t. Now it follows that there exists a temporal coordinate scale such that $v_r(t) \leq 1$ for all t.

Assumption 2: The relative distance between the robot and the i^{th} landmark at time t belongs to $d_i(t) \in (0, \infty)$ in any arbitrarily chosen coordinate scale. There exists a spatial coordinate scale such that for all t we have $d_i \in [1, \infty)$.

Assumptions 1 and 2 are weak (actually notational) and can almost surely be satisfied in practice (i.e. by finding explicit spatial and temporal scales). The case of $v_r = 0$ is trivially obtained from the subsequent results. For simplicity we also assume the following.

Assumption 3: For all t we have $\widehat{\mathbf{r}}_i(t) = [\widehat{d}_i(t)\ \widehat{\vartheta}_i(t)]^\top$ with $\widehat{d}_i \in [1, \infty)$ and $\widehat{\vartheta}_i \in [-\pi, \pi)$.

Assumption 4: For all t we assume that the error $\zeta_{i2} = (\vartheta_i - \widehat{\vartheta}_i)$ is taken modulo 2π and $\zeta_{i2} \in [-\pi, \pi)$.

Assumption 3 calls for the state estimate components to be restricted to the assumed true global state space. For $\widehat{\vartheta}_i(t)$ this can be achieved via a trivial modular operation. Assumption 4 ensures the value of the bearing error falls within a consistent 2π interval. Finally, we make the following standard assumption regarding the design parameters

Assumption 5: The following $\mathbf{Q}(t) \geq \underline{q}\mathbf{I}$, $\mathbf{R}(t) \geq \underline{r}\mathbf{I}$ and $\mathbf{P}(t_0) \geq p_0\mathbf{I}$ are given for some $\underline{q}, \underline{r}, p_0 > 0$ such that $\|\mathbf{Q}(t)\| \geq \underline{q}$ and $\|\mathbf{R}(t)\| \geq \underline{r}$. Moreover, $\mathbf{Q}(t)$ and $\mathbf{R}(t)$ are chosen to be bounded by $\|\mathbf{Q}(t)\| \leq \overline{q} < \infty$ and $\|\mathbf{R}(t)\| \leq \overline{r} < \infty$ for all t. Also, we have $\mathbf{E}(t) \leq \overline{e} < \infty$ with $\mathbf{E}(t) \geq \underline{e}\mathbf{I}$.

We will also need the following lemma concerning the growth of $\varrho(\mathbf{z}, \widehat{\mathbf{z}}, v_r, w_r)$.

Lemma 1: The following inequality holds

$$\begin{aligned} \|\varrho(\mathbf{z}, \widehat{\mathbf{z}}, v_r, w_r)\| &= \|f(\mathbf{z}, \cdot) - f(\widehat{\mathbf{z}}, \cdot) - \mathbf{A}(t)(\mathbf{z} - \widehat{\mathbf{z}})\| \\ &\leq 2\overline{a}\|\boldsymbol{\zeta}\| \end{aligned} \tag{21}$$

for $|\mathcal{V}| = n$ with probability 1 when Assumptions 1-5 hold.

Proof: From the triangle inequality we obtain

$$\begin{aligned}\|f(\mathbf{z},v_r,w_r)-f(\widehat{\mathbf{z}},v_r,w_r)-\mathbf{A}(t)(\mathbf{z}-\widehat{\mathbf{z}})\| &\leq \\ \|f(\mathbf{z},v_r,w_r)-f(\widehat{\mathbf{z}},v_r,w_r)\|+\|-\mathbf{A}(t)\boldsymbol{\zeta}\| &\leq \\ \|f(\mathbf{z},v_r,w_r)-f(\widehat{\mathbf{z}},v_r,w_r)\|+\overline{a}\boldsymbol{\zeta} & \quad (22)\end{aligned}$$

which follows using (19). Now if $f(\cdot)$ is Lipschitz then $\|f(\mathbf{z},v_r,w_r)-f(\widehat{\mathbf{z}},v_r,w_r)\|\leq c\|\mathbf{z}-\widehat{\mathbf{z}}\|$ for some $0<c<\infty$. Actually, we know that if $\|\mathbf{A}(t)\|$ is bounded by $\overline{a}$ then $f(\cdot)$ is Lipschitz with Lipschitz coefficient $\overline{a}$. Thus, the proof is immediate. ■

Note also that $\varrho(\mathbf{z},\widehat{\mathbf{z}},v_r,w_r)=0$ when $\boldsymbol{\zeta}(t)=0$. We now consider the the propagation of the estimation error $\boldsymbol{\zeta}(t)=\mathbf{z}(t)-\widehat{\mathbf{z}}(t)$ for all $t>t_0$ given an initial estimation error $\boldsymbol{\zeta}(t_0)$ which we will assume belongs to the set

$$\boldsymbol{\zeta}(t_0)=\{\boldsymbol{\eta}\in\{[0,\infty)\times[-\pi,\pi)\}:\|\boldsymbol{\zeta}(t_0)\|\leq b\} \quad (23)$$

for some constant $b<\infty$. We assume initially that $\mathcal{G}(t)=\mathcal{V}$ for all $t>t_0$. The error propagates according to (17) with (for simplicity) $\mathbf{H}(\mathcal{G}(t))=\mathbf{I}$ for all t. It is common to assume a full landmark measurement vector when performing such an analysis [4], [12]. We state the following lemma regarding the error covariance.

Lemma 2: Suppose Assumptions 1-5 hold. Then the state estimate covariance $\mathbf{P}(t)$ is bounded by

$$0<\underline{p}\leq\mathbf{P}(t)\leq\overline{p}<\infty \quad (24)$$

for all $t>t_0$ and where

$$\overline{p}\triangleq\left(\|\mathbf{P}(t_0)\|+\frac{\|\mathbf{Q}(t)\|+\|\mathbf{R}(t)\|\|\mathbf{\Lambda}(t)\|^2}{2\kappa}\right) \quad (25)$$

and where $\mathbf{\Lambda}$ is chosen such that

$$\boldsymbol{\eta}^\top\left(\mathbf{A}(t)+\mathbf{\Lambda}(t)\right)\boldsymbol{\eta}\leq-\kappa\|\boldsymbol{\eta}\|^2 \quad (26)$$

is satisfied for all $\boldsymbol{\eta}\in\mathbb{R}^2$ with $\kappa>0$.

Proof: The upper bound can be obtained by considering the following time-varying linear control system

$$-\dot{\mathbf{q}}=\mathbf{A}(t)\mathbf{q}+\mathbf{u} \quad (27)$$

with a boundary $\mathbf{q}(T)=\mathbf{q}_T$ for some $0<T\leq\infty$ and with controllability Grammian

$$\mathcal{C}(t+\tau,t)=\int_t^{t+\tau}\mathbf{\Psi}(t+\tau,t)\mathbf{\Psi}^\top(t+\tau,t)dt \quad (28)$$

where $\mathbf{\Psi}(t+\tau,t)$ is the fundamental matrix with $\mathbf{\Psi}(t,t)=\mathbf{I}$. The system (27) is uniformly completely controllable since $\|\mathbf{A}(t)\|<\infty$ and $\|\mathbf{\Psi}(t+\tau,t)\|>\exp(-\tau\|\mathbf{A}(t)\|)$ which implies $\mathcal{C}(t+\tau,t)$ is never singular for $t_0\leq t<\tau$. Consider the following cost function

$$\mathcal{J}(t,\tau,\mathbf{q},\mathbf{u})=\mathcal{B}(t_0,\mathbf{q}(t_0))+\int_{t_0}^T\left(\mathbf{q}^\top\mathbf{Q}\mathbf{q}+\mathbf{u}^\top\mathbf{R}\mathbf{u}\right)dt \quad (29)$$

and value function $\mathcal{B}(t,\mathbf{q}(t))=\mathbf{q}^\top(t)\mathbf{P}(t)\mathbf{q}(t)$. Let the control input equal $\mathbf{u}(t)=\mathbf{\Lambda}(t)\mathbf{q}$ for some continuous bounded matrix $\mathbf{\Lambda}(t)$ such that $-\dot{\mathbf{q}}=(\mathbf{A}(t)+\mathbf{\Lambda}(t))\,\mathbf{q}$. Note now that

$$\begin{aligned}\mathcal{B}(T,\mathbf{q}(T)) &= \mathbf{q}^\top(T)\mathbf{P}(T)\mathbf{q}(T)\\ &\leq \mathcal{B}(t_0,\mathbf{q}(t_0))+\\ &\quad\int_{t_0}^T\mathbf{q}^\top\left(\mathbf{Q}+\mathbf{\Lambda}^\top(t)\mathbf{R}\mathbf{\Lambda}(t)\right)\mathbf{q}dt \quad (30)\end{aligned}$$

Solving $-\dot{\mathbf{q}}=(\mathbf{A}(t)+\mathbf{\Lambda}(t))\,\mathbf{q}$ for $\mathbf{q}(T)$ implies that

$$\begin{aligned}\|\mathbf{q}(T)\|^2 &= \|\mathbf{q}_T\|^2=\|\mathbf{q}(t_0)\|^2-\\ &\quad 2\int_{t_0}^T\mathbf{q}^\top\left(\mathbf{A}(t)+\mathbf{\Lambda}(t)\right)\mathbf{q}\;dt \quad (31)\end{aligned}$$

and thus (26) implies that $\|\mathbf{q}(t_0)\|^2\leq\|\mathbf{q}_T\|^2$ and $\int_{t_0}^T\mathbf{q}^\top\mathbf{q}\leq\frac{\|\mathbf{q}_T\|^2}{2\kappa}$. Using this with (30) leads easily to the upper-bound. ■

Note that $\|\mathbf{P}(t)\|$ is bounded above by a constant independent of the time $t>t_0$. This bound holds irrespective of whether or not the state estimation error is bounded. Part of Lemma 2 follows from a theorem given in [21]. The condition (26) calls for the system pair $\mathbf{A}(t)$ and $\mathbf{H}(\mathcal{G}(t))=\mathbf{I}$ to be uniformly detectable. In our case we know that the system is observable (which implies detectability [21], [22]). As such, a suitable matrix $\mathbf{\Lambda}(t)$ exists with probability one. Alternatively, an upper-bound on $\|\mathbf{P}(t)\|$ can be derived independent of (26) when the state is observable [21].

We now state a result concerning the exponential boundedness of the expected error $\mathcal{E}\{\|\boldsymbol{\zeta}(t)\|\}$ for all $t>t_0$ and the asymptotic properties of the expected estimation error.

Theorem 1: Consider the system (17) with an initial condition (23) and $\mathbf{H}(\mathcal{G}(t))=\mathbf{I}$. Suppose that Assumptions 1-5 hold. If $\|\mathbf{P}^{-1}(t)\mathbf{Q}(t)\mathbf{P}^{-1}(t)+\mathbf{R}^{-1}(t)\|\underline{p}>\frac{4\overline{ap}}{\underline{p}}$ then the estimation error is bounded above with

$$\mathcal{E}\left\{\|\boldsymbol{\zeta}(t)\|^2\right\}\leq\max\left\{\frac{n\overline{pe}^2}{2\gamma\underline{r}^2},\;\frac{\overline{p}}{\underline{p}}\|\boldsymbol{\zeta}(t_0)\|^2\right\} \quad (32)$$

where $\gamma=\|\mathbf{P}^{-1}(t)\mathbf{Q}(t)\mathbf{P}^{-1}(t)+\mathbf{R}^{-1}(t)\|\underline{p}-4\overline{ap}/\underline{p}$ and the error $\mathcal{E}\left\{\|\boldsymbol{\zeta}(t)\|^2\right\}$ as $t\to\infty$ is bounded by $\frac{n\overline{pe}^2}{2\gamma\underline{r}^2}$.

Proof: The error system (17) can be thought of as a linear system with a nonlinear perturbation being driven by a zero-mean Weiner process. Let $\mathcal{B}(t,\boldsymbol{\zeta}(t))=\boldsymbol{\zeta}^\top(t)\mathbf{P}^{-1}(t)\boldsymbol{\zeta}(t)>0$ and note that

$$\begin{aligned}d\mathcal{B} &= \left[\frac{\partial\mathcal{B}}{\partial t}+\frac{\partial\mathcal{B}}{\partial\boldsymbol{\zeta}}\left(\mathbf{A}(t)-\mathbf{K}(t)\right)\boldsymbol{\zeta}\right]dt+\\ &\quad\frac{\partial\mathcal{B}}{\partial\boldsymbol{\zeta}}\varrho(\mathbf{z},\widehat{\mathbf{z}},v_r,w_r)dt+\\ &\quad\frac{1}{2}\mathrm{tr}\left(\mathrm{hess}(\mathcal{B})\mathbf{K}(t)\mathbf{E}(t)\mathbf{E}^\top(t)\mathbf{K}^\top(t)\right)dt-\\ &\quad\frac{\partial\mathcal{B}}{\partial\boldsymbol{\zeta}}\mathbf{K}(t)\mathbf{E}(t)d\mathbf{n}\\ d\mathcal{B} &= \left[\frac{\partial\mathcal{B}}{\partial t}+\mathcal{L}\mathcal{B}\right]dt-\frac{\partial\mathcal{B}}{\partial\boldsymbol{\zeta}}\mathbf{K}(t)\mathbf{E}(t)d\mathbf{n} \quad (33)\end{aligned}$$

using Ito's differential formula and where $\mathcal{L}$ is the Kolmogorov backward operator, $\mathrm{hess}(\cdot)$ denotes the Hessian operator and $\mathrm{tr}(\cdot)$ denotes the matrix trace. Evaluating the terms and re-arranging leads to

$$
\begin{aligned}
d\mathcal{B} &= \Big[\boldsymbol{\zeta}^\top \left[\mathbf{P}^{-1}(t)\mathbf{Q}(t)\mathbf{P}^{-1}(t)+\mathbf{R}^{-1}(t)\right]\boldsymbol{\zeta}\Big] dt + \\
&\quad 2\boldsymbol{\zeta}^\top \mathbf{P}^{-1}(t)\varrho(\mathbf{z},\widehat{\mathbf{z}},v_r,w_r)dt + \\
&\quad \frac{1}{2}\mathrm{tr}\left(\mathbf{R}^{-1}(t)\mathbf{E}(t)\mathbf{E}(t)\mathbf{R}^{-\top}(t)\mathbf{P}^\top(t)\right)dt - \\
&\quad 2\boldsymbol{\zeta}^\top\mathbf{R}^{-1}(t)d\mathbf{n} \\
&\leq \left[-\alpha\|\boldsymbol{\zeta}\|^2 + \frac{4\overline{a}}{\underline{p}}\|\boldsymbol{\zeta}\|^2 + \frac{n\overline{pe}^2}{2\underline{r}^2}\right]dt - \\
&\quad 2\boldsymbol{\zeta}^\top\mathbf{R}^{-1}(t)d\mathbf{n} \qquad (34)
\end{aligned}
$$

where we have explicitly employed Lemma 1 and Lemma 2 and where

$$\alpha = \|\mathbf{P}^{-1}(t)\mathbf{Q}(t)\mathbf{P}^{-1}(t)+\mathbf{R}^{-1}(t)\| \qquad (35)$$

Clearly we have $\overline{p}^{-1}\|\boldsymbol{\zeta}\|^2 \leq \mathcal{B}(t,\boldsymbol{\zeta}(t)) \leq \underline{p}^{-1}\|\boldsymbol{\zeta}\|^2$ such that some simple algebra implies that

$$
\begin{aligned}
d\mathcal{B} &\leq -\left(\alpha\underline{p} - \frac{4\overline{ap}}{\underline{p}}\right)\mathcal{B}dt + \frac{n\overline{pe}^2}{2\underline{r}^2}dt - \\
&\quad 2\boldsymbol{\zeta}^\top\mathbf{R}^{-1}(t)d\mathbf{n} \\
\mathcal{B} &\leq \mathcal{B}(t_0,\boldsymbol{\zeta}(t_0)) - \\
&\quad \int_{t_0}^t \left(\alpha\underline{p} - \frac{4\overline{ap}}{\underline{p}}\right)\mathcal{B}(\tau,\boldsymbol{\zeta}(\tau))d\tau + \\
&\quad \frac{n\overline{pe}^2}{2\underline{r}^2}\int_{t_0}^t d\tau - 2\int_{t_0}^t \boldsymbol{\zeta}^\top(\tau)\mathbf{R}^{-1}(\tau)d\mathbf{n}(\tau) \quad (36)
\end{aligned}
$$

From the Bellman-Gromwall lemma [23] we have

$$
\begin{aligned}
\mathcal{B}(t,\boldsymbol{\zeta}(t)) &\leq \mathcal{B}(t_0,\boldsymbol{\zeta}(t_0))\exp\left(-\gamma(t-t_0)\right) + \\
&\quad \frac{n\overline{pe}^2}{2\gamma\underline{r}^2}\left(1-\exp\left(-\gamma(t-t_0)\right)\right) - \\
&\quad 2\int_{t_0}^t \boldsymbol{\zeta}^\top(\tau)\mathbf{R}^{-1}(\tau)d\mathbf{n}(\tau) \qquad (37)
\end{aligned}
$$

where

$$\gamma = \left(\alpha\underline{p} - 4\overline{ap}/\underline{p}\right) \qquad (38)$$

with $\gamma > 0$ if and only if $\alpha\underline{p} > \frac{4\overline{ap}}{\underline{p}}$. Taking the expectation $\mathcal{E}\{\cdot\}$ of both sides of (37) gives

$$
\begin{aligned}
\mathcal{E}\left\{\mathcal{B}(t,\boldsymbol{\zeta}(t))\right\} &\leq \mathcal{B}(t_0,\boldsymbol{\zeta}(t_0))\exp\left(-\gamma(t-t_0)\right) + \\
&\quad \frac{n\overline{pe}^2}{2\gamma\underline{r}^2}\left(1-\exp\left(-\gamma(t-t_0)\right)\right) \quad (39)
\end{aligned}
$$

and thus

$$
\begin{aligned}
\mathcal{E}\left\{\|\boldsymbol{\zeta}(t)\|^2\right\} &\leq \frac{\overline{p}}{\underline{p}}\|\boldsymbol{\zeta}(t_0)\|^2\exp\left(-\gamma(t-t_0)\right) + \\
&\quad \frac{n\overline{pe}^2}{2\gamma\underline{r}^2}\left(1-\exp\left(-\gamma(t-t_0)\right)\right) \quad (40)
\end{aligned}
$$

We then easily find that

$$\mathcal{E}\left\{\|\boldsymbol{\zeta}(t)\|^2\right\} \leq \max\left\{\frac{n\overline{pe}^2}{2\gamma\underline{r}^2},\ \frac{\overline{p}}{\underline{p}}\|\boldsymbol{\zeta}(t_0)\|^2\right\} \qquad (41)$$

for all t if $\gamma > 0$ and the error $\mathcal{E}\left\{\|\boldsymbol{\zeta}(t)\|^2\right\}$ as $t \to \infty$ is bounded by $\frac{n\overline{pe}^2}{2\gamma\underline{r}^2}$. This completes the proof. ∎

Importantly, we have shown under what conditions an EKF-like algorithm will yield an exponentially bounded and converging mean-square estimation error. The condition $\gamma > 0$, which guarantees the expected error converges, is independent of $\overline{e}$. We have also given a method of estimating the asymptotic mean-square error. The asymptotic mean-square estimation error is dependent on the specific robot trajectory but is upper-bounded by $\frac{n\overline{pe}^2}{2\gamma\underline{r}^2}$. Theorem 1 is a significant contribution to the problem of robocentric mapping and is a fundamental result. It is important to note again that the algorithm considered in this paper is based on nothing more than an EKF-like architecture and a coordinate transform; see [20], [24], [25] for other EKF stability results.

3) Noisy Robot-Landmark Dynamics and Noisy Measurements: We now consider the case where process noise is present and where (for simplicity) $\mathbf{H}(\mathcal{G}(t)) = \mathbf{I}$ for all t. We assume an EKF-like algorithm of the form (12) with Assumptions 1-5 holding. The error $\boldsymbol{\zeta} = \mathbf{z} - \widehat{\mathbf{z}}$ obeys

$$
\begin{aligned}
d\boldsymbol{\zeta} &= \left[\left(\mathbf{A}(t)-\mathbf{K}(t)\right)\boldsymbol{\zeta} + \varrho(\mathbf{z},\widehat{\mathbf{z}},v_r,w_r)\right]dt + \\
&\quad \mathbf{G}(t)\begin{bmatrix} dv \\ dw \end{bmatrix} - \mathbf{K}(t)\mathbf{E}(t)d\mathbf{n}(t) \\
d\boldsymbol{\zeta} &= \left[\left(\mathbf{A}(t)-\mathbf{K}(t)\right)\boldsymbol{\zeta} + \varrho(\mathbf{z},\widehat{\mathbf{z}},v_r,w_r)\right]dt + \\
&\quad \left[\mathbf{G}(t) \ \ -\mathbf{K}(t)\mathbf{E}(t)\right]\begin{bmatrix} \begin{bmatrix} dv \\ dw \end{bmatrix} \\ d\mathbf{n}(t) \end{bmatrix} \qquad (42)
\end{aligned}
$$

where $\mathbf{G}_i(t)$ is given by

$$\|\mathbf{G}_i(t)\| = \left\|\begin{bmatrix} \sigma_v\cos\vartheta_i & 0 \\ \sigma_v\sin\vartheta_i & -\sigma_w \end{bmatrix}\right\| = \overline{g} < \infty \qquad (43)$$

and $\mathbf{G}(t) = \left[\mathbf{G}_1(t) \ \ldots \ \mathbf{G}_n(t)\right]^\top$. Moreover, Lemma 1 and Lemma 2 still apply since they depend only on the validity of Assumptions 1-5. Now we are in a position to prove the main result concerning the exponential boundedness of the expected estimation error for all $t > t_0$.

Theorem 2: Consider the system (42) with an initial condition (23) and $\mathbf{H}(\mathcal{G}(t)) = \mathbf{I}$. Suppose that Assumptions 1-5 hold. If $\|\mathbf{P}^{-1}(t)\mathbf{Q}(t)\mathbf{P}^{-1}(t)+\mathbf{R}^{-1}(t)\|\underline{p} > \frac{4\overline{ap}}{\underline{p}}$ then the estimation error is bounded above with

$$\mathcal{E}\left\{\|\boldsymbol{\zeta}(t)\|^2\right\} \leq \max\left\{\frac{n(\underline{r}^2\overline{g}^2+\overline{p}\overline{pe}^2)}{2\gamma\underline{r}^2\underline{p}},\ \frac{\overline{p}}{\underline{p}}\|\boldsymbol{\zeta}(t_0)\|^2\right\} \quad (44)$$

where $\gamma = \|\mathbf{P}^{-1}(t)\mathbf{Q}(t)\mathbf{P}^{-1}(t)+\mathbf{R}^{-1}(t)\|\underline{p} - 4\overline{ap}/\underline{p}$ and the error $\mathcal{E}\left\{\|\boldsymbol{\zeta}(t)\|^2\right\}$ as $t \to \infty$ is bounded by $\frac{n(\underline{r}^2\overline{g}^2+\overline{p}\overline{pe}^2)}{2\gamma\underline{r}^2\underline{p}}$.

Proof: The proof is similar to the proof of Theorem 1. We will omit most of the details as a consequence. Let $\mathcal{B}(t,\boldsymbol{\zeta}(t)) = \boldsymbol{\zeta}^\top(t)\mathbf{P}^{-1}(t)\boldsymbol{\zeta}(t) > 0$ and note that

$$
\begin{aligned}
d\mathcal{B} &= \left[\frac{\partial\mathcal{B}}{\partial t} + \frac{\partial\mathcal{B}}{\partial\boldsymbol{\zeta}}\left(\mathbf{A}(t)-\mathbf{K}(t)\right)\boldsymbol{\zeta} + \frac{\partial\mathcal{B}}{\partial\boldsymbol{\zeta}}\varrho(\mathbf{z},\widehat{\mathbf{z}},\cdot)\right]dt + \\
&\quad dt + \\
&\quad \frac{1}{2}\mathrm{tr}\left(\mathrm{hess}(\mathcal{B})\boldsymbol{\Xi}(t)\boldsymbol{\Xi}^\top(t)\right)dt - \\
&\quad \frac{\partial\mathcal{B}}{\partial\boldsymbol{\zeta}}\boldsymbol{\Xi}(t)\begin{bmatrix} \begin{bmatrix} dv \\ dw \end{bmatrix} \\ d\mathbf{n}(t) \end{bmatrix} \qquad (45)
\end{aligned}
$$

where

$$\boldsymbol{\Xi}(t) = [\mathbf{G}(t) \ -\mathbf{K}(t)\mathbf{E}(t)] \quad (46)$$

and where we have employed Itos differential formula. Evaluating the terms and re-arranging leads to

$$\begin{aligned} d\mathcal{B} &= \left[\boldsymbol{\zeta}^\top \left[\mathbf{P}^{-1}(t)\mathbf{Q}(t)\mathbf{P}^{-1}(t) + \mathbf{R}^{-1}(t)\right]\boldsymbol{\zeta}\right] dt + \\ & 2\boldsymbol{\zeta}^\top \mathbf{P}^{-1}(t)\varrho(\mathbf{z}, \widehat{\mathbf{z}}, v_r, w_r) dt + \\ & \frac{1}{2}\mathrm{tr}\left(\mathbf{P}^{-1}(t)\mathbf{G}(t)\mathbf{G}^\top(t)\right) dt + \\ & \frac{1}{2}\mathrm{tr}\left(\mathbf{P}^{-1}(t)\mathbf{K}(t)\mathbf{K}^\top(t)\right) dt - \\ & 2\boldsymbol{\zeta}^\top \mathbf{P}^{-1}(t)\boldsymbol{\Xi}(t)\left[\begin{array}{c}\left[\begin{array}{c} dv \\ dw \end{array}\right] \\ d\mathbf{n}(t)\end{array}\right] \\ &\leq \left[-\alpha\|\boldsymbol{\zeta}\|^2 + \frac{4\overline{a}}{\underline{p}}\|\boldsymbol{\zeta}\|^2 + \frac{n(\underline{r}^2\overline{g}^2 + \overline{p}\underline{p}\overline{e}^2)}{2\gamma\underline{r}^2\underline{p}}\right] dt - \\ & 2\boldsymbol{\zeta}^\top \mathbf{P}^{-1}(t)\boldsymbol{\Xi}(t)\left[\begin{array}{c}\left[\begin{array}{c} dv \\ dw \end{array}\right] \\ d\mathbf{n}(t)\end{array}\right] \end{aligned} \quad (47)$$

where we have explicitly employed Lemma 1 and Lemma 2 and where

$$\alpha = \|\mathbf{P}^{-1}(t)\mathbf{Q}(t)\mathbf{P}^{-1}(t) + \mathbf{R}^{-1}(t)\| \quad (48)$$

Now noting that $\overline{p}^{-1}\|\boldsymbol{\zeta}\|^2 \leq \mathcal{B}(t, \boldsymbol{\zeta}(t)) \leq \underline{p}^{-1}\|\boldsymbol{\zeta}\|^2$ and using the Bellman-Gromwall lemma [23] we come to

$$\begin{aligned} \mathcal{B}(t, \boldsymbol{\zeta}(t)) &\leq \mathcal{B}(t_0, \boldsymbol{\zeta}(t_0)) \exp\left(-\gamma(t - t_0)\right) - \\ & 2\int_{t_0}^{t} \boldsymbol{\zeta}^\top(\tau)\mathbf{P}^{-1}(\tau)\boldsymbol{\Xi}(\tau)\left[\begin{array}{c}\left[\begin{array}{c} dv(\tau) \\ dw(\tau) \end{array}\right] \\ d\mathbf{n}(\tau)\end{array}\right] + \\ & \frac{n(\underline{r}^2\overline{g}^2 + \overline{p}\underline{p}\overline{e}^2)}{2\gamma\underline{r}^2\underline{p}} - \\ & \frac{n(\underline{r}^2\overline{g}^2 + \overline{p}\underline{p}\overline{e}^2)}{2\gamma\underline{r}^2\underline{p}} \exp\left(-\gamma(t - t_0)\right) \end{aligned} \quad (49)$$

where

$$\gamma = \left(\alpha\underline{p} - 4\frac{\overline{ap}}{\underline{p}}\right) \quad (50)$$

with $\gamma > 0$ if and only if $\alpha\underline{p} > \frac{4\overline{ap}}{\underline{p}}$. Taking the expectation of (49) and proceeding as in the proof of Theorem 1 gives

$$\mathcal{E}\left\{\|\boldsymbol{\zeta}(t)\|^2\right\} \leq \max\left\{\frac{n(\underline{r}^2\overline{g}^2 + \overline{p}\underline{p}\overline{e}^2)}{2\gamma\underline{r}^2\underline{p}}, \ \frac{\overline{p}}{\underline{p}}\|\boldsymbol{\zeta}(t_0)\|^2\right\} \quad (51)$$

for all t if $\gamma > 0$. The error $\mathcal{E}\left\{\|\boldsymbol{\zeta}(t)\|^2\right\}$ as $t \to \infty$ is bounded by $\frac{n(\underline{r}^2\overline{g}^2 + \overline{p}\underline{p}\overline{e}^2)}{2\gamma\underline{r}^2\underline{p}}$. This completes the proof. ■

Again we have a fundamental result concerning the exponential boundedness and convergence of the expected estimation error. Note that the steady state expected mean square error bound is larger when process noise is present (as expected).

IV. Numerical Simulations

The algorithm presented in this paper is now illustrated via simulation. The examples we consider involve a single mobile robot and a rectangular configuration of 40 landmarks. The scenario is illustrated graphically in Figure 1.

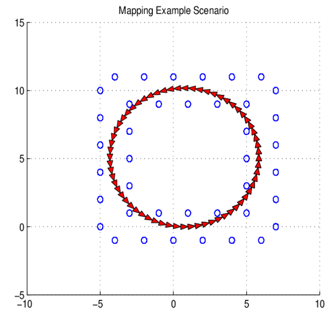

Fig. 1. The example scenario considered in this paper consists of 40 landmarks and a single mobile robot. The true robot trajectory is illustrated by the sequence of arrow heads (and starts at the origin).

The true robot velocity has a magnitude $v_r = 0.5$. The true angular velocity of the robot has magnitude $w_r = \frac{\pi}{32}$. The matrix $\mathbf{Q}(t) = \mathbf{G}(t)\mathbf{G}^\top(t)$ is evaluated at the estimated target state but uses the true values of σ_v and σ_w. The matrix $\mathbf{R}$ is a constant matrix representing the true covariance of the measurement vector. The initial landmark positions are equal to the first noisy measurements and the associated initial covariance matrix is equal to $\mathbf{R}$. This initialization method is a very convenient side benefit of our approach.

A. Example 1

Firstly we consider the case in which the robot senses the entire set $\mathcal{V}$ of landmarks for all t. This is of course not entirely practical but is the precise condition under which the analysis of this paper pertains to (and is a common assumption made when analyzing the convergence of mapping and/or SLAM algorithms). The velocity error has standard deviation magnitude of $\sigma_v = 0.05$. The angular acceleration error has a standard deviation magnitude of $\sigma_w = 0.0175$. The bearing and range noise are assumed to be independent of the state with standard deviation magnitudes of 0.035 and 0.5 respectively. The RMS state estimation error for 10000 simulation runs is shown in Figure 2.

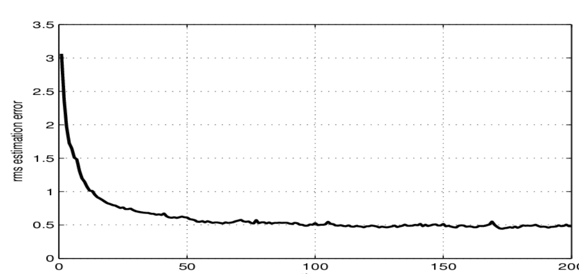

Fig. 2. The RMS state estimation error for the complete relative (robocentric) range and bearing state estimate for example 1.

It is clear that the error is bounded above and converging to a steady value. Note that the error vector consists of bearing and range errors (as we are working in polar coordinates). However, each state component is bounded and convergent. The error covariance also converges and we plot the average maximum singular value of $\mathbf{P}(t)$ in Figure 3.

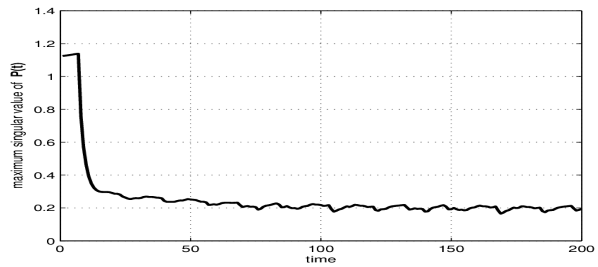

Fig. 3. The average maximum singular value of $\mathbf{P}(t)$ for example 1.

It is clear that the maximum singular value of the covariance matrix $\mathbf{P}(t)$ converges very fast to a steady state value. The average value of α and $\|\mathbf{A}(t)\|$ is shown in Figure 4.

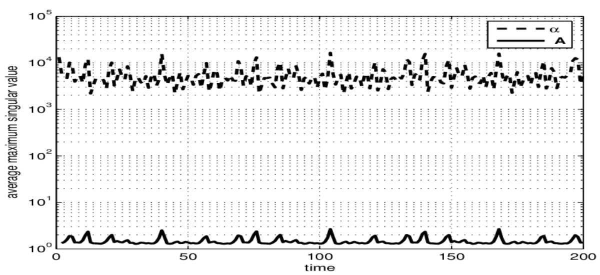

Fig. 4. The mean value of α and $\|\mathbf{A}(t)\|$ for example 1.

From Figure 3 and Figure 4 we can verify that the simulation results agree with the theoretical results provided in this paper.

B. Example 2

The example considered here is identical to the previous example except for the values of the noise variances. Here we increase the values such that $\sigma_v = 0.1$ and $\sigma_w = 0.035$. The bearing and range noise standard deviations are 0.175 and 1.5 respectively. These are large error statistics. The RMS state error value for 10000 simulation runs is shown in Figure 5.

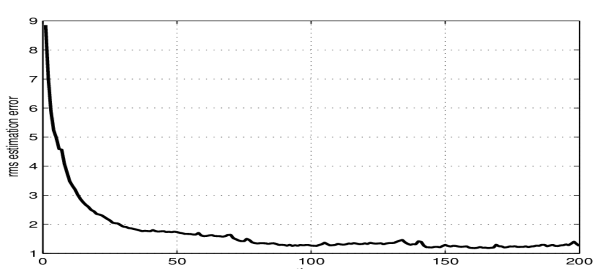

Fig. 5. The RMS state estimation error for the complete relative (robocentric) range and bearing state estimate for example 2.

The RMS error is bounded above and converging. The value to which the error is converging is also greater than that value indicated in Figure 2 for example 1 (as expected) and it takes slightly longer for the error to reach a steady-value. The covariance matrix $\mathbf{P}(t)$ or more specifically $\|\mathbf{P}(t)\|$ also converges to a steady state value as expected. It can similarly be shown (as was the case in example 1) that the condition $\gamma > 0$ is satisfied in this simulation example (given relatively large error statistics).

A significant advantage exhibited by the algorithm considered in this paper is the coordinate transformation that subsequently permits linear measurements. This can considerably improve the performance of the EKF as shown here and in the bearing-only tracking literature [19], [20].

C. Example 3

Finally, we consider the same noise parameters and simulation scenario as examined in example 1 but we restrict the sensing domain of the robot such that it can only sense a subset $\mathcal{G} \subseteq \mathcal{V}$ of landmarks at each time t. Specifically, the robot can sense a landmark i at time s if and only if $\vartheta_i(s) \in (-\pi/2, \pi/2)$ and $d_i(s) \in (0, 5)$. We assume perfect data-association capabilities. The duration of each simulation run is increased to 400 seconds. We plot the RMS state error value over 10000 simulation runs in Figure 6.

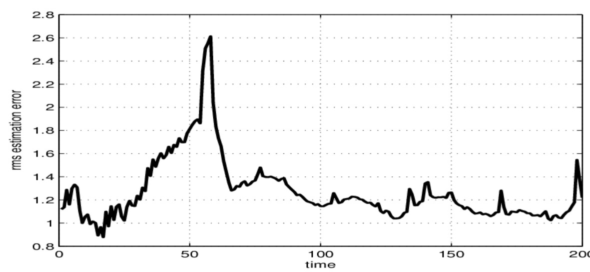

Fig. 6. The RMS state estimation error for the complete relative (robocentric) range and bearing state estimate for example 3.

The robot completes one cycle and closes-the-loop in just over 50 seconds. The error is increasing as the robot moves from its initial position at the origin around the first loop. When the robot completes one loop we see a notable (and sudden) decrease in the error which then converges to a reasonably stable value. We plot the average maximum singular value of $\mathbf{P}(t)$ in Figure 7.

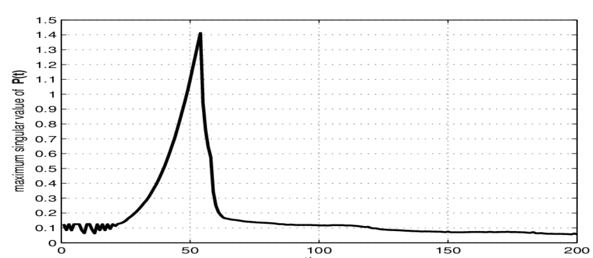

Fig. 7. The average maximum singular value of $\mathbf{P}(t)$ for example 3.

A similar situation is observed with the singular values of the covariance matrix $\mathbf{P}(t)$. During the first loop the uncertainty is increasing and following the loop-closure the uncertainty decreases dramatically.

V. DISCUSSION

Consider the state variable $\mathbf{z} = [\mathbf{s}_r \ \mathbf{r}_1 \ \dots \ \mathbf{r}_n]^\top$ and the corresponding EKF algorithm used to estimate $\mathbf{z}$. The state estimation of the subspace $[\mathbf{r}_1 \ \dots \ \mathbf{r}_n]^\top$ would obey the analytical results derived in this paper while the state estimation of $[\mathbf{s}_r]$ would depend on the nonlinear measurements and is not covered explicitly in this paper. Actually, $[\mathbf{s}_r]$ represents an unobservable subspace of $\mathbf{z} = [\mathbf{s}_r \ \mathbf{r}_1 \ \dots \ \mathbf{r}_n]^\top$. Thus it is possible to directly relate the robocentric mapping algorithm developed in this paper to the general global SLAM problem by simply further augmenting the state variable as $\mathbf{z} = [\mathbf{s}_r \ \mathbf{r}_1 \ \dots \ \mathbf{r}_n]^\top$ and modifying (in an obvious way) certain properties of the EKF algorithm. The result would be an algorithm for an unobservable state variable. The observable state space $[\mathbf{r}_1 \ \dots \ \mathbf{r}_n]^\top$ is the robocentric output and the estimation error associated with the space $[\mathbf{r}_1 \ \dots \ \mathbf{r}_n]^\top$ would obey the results developed in this paper. Of course the entire state $\mathbf{z}$ might diverge and there is no guarantee that the entire $\mathbf{P}(t)$ matrix is bounded (this would depend non-trivially on the robot trajectory and initialization).

Further experimental and simulation results will appear in an extended version of this paper. The results given here were simplified in an attempt to highlight the main convergence properties of the filter. A comparison of the proposed algorithm with that of the traditional formulation of EKF-SLAM is warranted along with an analysis of the *degree-of-nonlinearity* of the converted dynamic model.

VI. CONCLUDING REMARKS

Robocentric mapping provides an attractive and tractable solution to many problems in robotics. The approach introduced in this paper is based on nothing more than an extended Kalman filter (EKF) and a very advantageous coordinate transform. The novelty of this transformation is that it leads to a linear measurement equation, i.e. it removes significant nonlinearities associated with the measurements. The standard unicycle model is given in polar coordinates and relative to each landmark position. Hence, the robocentric mapping problem given range and bearing measurements is formulated in (arguably) its most natural form. To justify the application of the EKF we then analyzed the finite-time and the asymptotic convergence properties of the error. We showed how the performance of the EKF estimation error can be related to the design parameters and the noise properties.

REFERENCES

[1] R. Smith, M. Self, and P. Cheeseman. Estimating uncertain spatial relationships in robotics. *Autonomous Robot Vehicles*, pages 167–193, Springer-Verlag 1990.

[2] H. F. Durrant-Whyte. Uncertain geometry in robotics. *IEEE Transactions on Robotics and Automation*, 4:23–31, 1988.

[3] S. Thrun, D. Fox, and W. Burgard. A probabilistic approach to concurrent mapping and localization for mobile robots. *Mach. Learning Autonom. Robots*, 31:29–53, 1998.

[4] M.W.M.G. Dissanayake, P. Newman, S. Clark, H.F. Durrant-Whyte, and M. Csorba. A solution to the simultaneous localization and map building (SLAM) problem. *IEEE Transactions on Robotics and Automation*, 17(3):229–241, June 2001.

[5] Estrada C., Neira J., and Tardos J.D. Hierarchical SLAM: Real-time accurate mapping of large environments. *IEEE Transactions on Robotics*, 21(4):588–596, August 2005.

[6] Walter M.R., Eustice R.M., and Leonard J.J. Exactly sparse extended information filters for feature-based SLAM. *International Journal of Robotics Research*, 26(4):335–359, April 2007.

[7] H. Durrant-Whyte and T. Bailey. Simultaneous localization and mapping (SLAM): Part I: The essential algorithms. *IEEE Robotics & Automation Magazine*, 13(2):99–108, 2006.

[8] T. Bailey and H. Durrant-Whyte. Simultaneous localization and mapping (SLAM): Part II: State of the art. *IEEE Robotics & Automation Magazine*, 13(3):108–117, 2006.

[9] G.P. Huang, A.I. Mourikis, and S.I. Roumeliotis. Analysis and improvement of the consistency of extended Kalman filter based SLAM. In *Proceedings of the 2008 International Conference on Robotics and Automation (ICRA)*, pages 473–479, May 2008.

[10] S.J. Julier and J.K. Uhlmann. A counter example to the theory of simultaneous localization and map building. In *Proceedings of the 2001 International Conference on Robotics and Automation (ICRA)*, pages 4238–4243, May 2001.

[11] T. Bailey, J. Nieto, J. Guivant, M. Stevens, and E. Nebot. Consistency of the EKF-SLAM algorithm. In *Proceedings of the 2006 IEEE/RSJ International Conference on Intelligent Robots and Systems (IROS)*, page 35623568, October 2006.

[12] S. Huang and G. Dissanayake. Convergence and consistency analysis for extended kalman filter based SLAM. *IEEE Transactions on Robotics*, 23(5):1036–1049, October 2007.

[13] Castellanos J.A., Martinez-Cantin R., Tardos J.D., and Neira J. Robocentric map joining: Improving the consistency of EKF-SLAM. *Robotics and Autonomous Systems*, 55(1):21–29, January 2007.

[14] F. Bourgault, A.A. Makarenko, S.B. Williams, B. Grocholsky, , and H.F. Durrant-Whyte. Information based adaptive robotic exploration. In *Proceedings of the 2002 IEEE/RSJ International Conference on Intelligent Robots and Systems (IROS)*, 2002.

[15] B. Grocholsky, J. Keller, V. Kumar, and G. Pappas. Cooperative air and ground surveillance. *IEEE Robotics & Automation Magazine*, 13(3):16–25, September 2006.

[16] A.N. Bishop, B. Fidan, B.D.O. Anderson, K. Dogancay, and P.N. Pathirana. Optimality analysis of sensor-target geometries in passive localization: Part 1 - Bearing-only localization. In *Proceedings of the 3rd International Conference on Intelligent Sensors, Sensor Networks and Information Processing (ISSNIP)*, December 2007.

[17] A.N. Bishop, B. Fidan, B.D.O. Anderson, P.N. Pathirana, and K. Dogancay. Optimality analysis of sensor-target geometries in passive localization: Part 2 - Time-of-arrival based localization. In *Proceedings of the 3rd International Conference on Intelligent Sensors, Sensor Networks and Information Processing (ISSNIP)*, December 2007.

[18] A.N. Bishop, B. Fidan, K. Dogancay, B.D.O. Anderson, and P.N. Pathirana. Exploiting geometry for improved hybrid AOA/TDOA based localization. *Signal Processing*, 88(7):17751791, July 2008.

[19] V. Aidala and S. Hammel. Utilization of modified polar coordinates for bearings-only tracking. *IEEE Transactions on Automatic Control*, 28(3):283294, March 1983.

[20] T. Song and J. Speyer. A stochastic analysis of a modified gain extended Kalman filter with applications to estimation with bearings only measurements. *IEEE Transactions on Automatic Control*, 30(10):940949, October 1985.

[21] J.S. Baras, A. Bensoussan, and M.R. James. Dynamic observers as asymptotic limits of recursive filters: Special cases. *SIAM Journal on Applied Mathematics*, 48(5):11471158, October 1988.

[22] B.D.O. Anderson and J.B. Moore. *Optimal Control: Linear Quadratic Methods*. Prentice-Hall, Englewood Cliffs, N.J., 1989.

[23] S. Sastry. *Nonlinear Systems: Analysis, Stability and Control*. Springer-Verlag, New York, N.Y., 1999.

[24] K. Reif, S. Gunther, E. Yaz, , and R. Unbehauen. Stochastic stability of the discrete-time extended Kalman filter. *IEEE Transactions on Automatic Control*, 44(4):714728, April 1999.

[25] K. Reif, S. Gunther, E. Yaz, , and R. Unbehauen. Stochastic stability of the continuous-time extended Kalman filter. *IEE Proceedings - Control Theory and Applications*, 147(1):4552, January 2000.